System Realization Using 2-D Output Measurements

J.E. Piou
Massachusetts Institute of Technology
Lincoln Laboratory

***Abstract*—A two-dimensional (2-D) system realization via output measurements is developed. The technique is based on multi-input multi-output (MIMO) systems where two sets of matrices *(A,B,C)* that characterize the system dynamics of a target in a 2-D space are obtained from the row and column directions of the output measurements. A modal decomposition approach is used to couple the two sets of matrices and obtain the states pairing without effort. Effectiveness of the technique is confirmed, and results are presented for static-range radar measurements taken on a canonical target.**

I. Introduction

System realization is a problem of considerable interest in many areas of control and signal processing. In recent years, system identification based on 1-D input-output data has received a lot of attention for applications in active control of flexible structures—mobile communications such as cellular and cordless telephony. In applications such as synthetic aperture of radar imaging, target identification of ballistic missiles, and determination of protein structure from nuclear magnetic resonance (NMR) that use only 2-D output data sets, system identification is rarely investigated. The two-dimensional nature of the problem and the absence of the input data make system identification a challenging task. However, Kung et al. [1] developed a method that can be regarded as a 2-D system realization. Reference [1] describes an efficient method for computing the state-space matrices from a 2-D output data set by exploiting the structure inherent in the measurements. However, in this approach the 2-D system realization is obtained from two separate sets of 1-D systems. The technique breaks down if either one or both open-loop matrices present multiple eigenvalues; moreover, the coupling of the two 1-D "system realizations" is not fully addressed.

In this paper, the matrix-enhanced and matrix pencil (MEMP) technique presented by Hua [2] is followed and the structure inherent in the data matrix proposed in Reference [1] is exploited to develop a novel 2-D system realization method. The technique is based on the open-loop matrices of two separate multi-input multi-output (MIMO) systems that are coupled via a modal decomposition carried on one of the open-loop matrices to obtain the state pair at no cost. The resulting technique provides enhanced 2-D state estimates. Under certain circumstances the 2-D system realization algorithm yields asymptotically unbiased minimum variance estimates. It is tested on static-range radar measurements taken on a canonical target.

The remainder of the paper is organized as follows: Section II describes the 2-D output data formulation, Section III presents a mathematical framework for the MIMO systems, Section IV describes the coupling of the two 1-D system realizations that gives rise to the 2-D system realization technique, and Section V presents results from static-range output measurements collected on a canonical target. Conclusions are presented in Section VI.

II. 2-D Output Data Formulation

It is assumed here that the 2-D data samples $y(m,n)$ corrupted with white Gaussian noise $w(m,n)$ have the following form:

$$y(m,n) = \sum_{i=1}^{P} a_i s_i^m p_i^n + w(m,n); \quad m = 1,\cdots,M; n = 1,\cdots,N \tag{1}$$

where *P* denotes the number of scatterers imbedded in the data; a_i refers to the *i*th complex amplitude associated with the *i*th scattering center with pole pair (s_i, p_i) and is defined by

$$a_i = |a_i| e^{j\phi_i}, \tag{2}$$

where ϕ_i denotes the *i*th phase. The poles s_i and p_i are obtained from the eigenvalues of the open-loop matrices

This research effort was supported under the auspices of the Lincoln Laboratory New Technology Initiatives Program. The New Technology Initiatives Program is supported principally by the Department of the Air Force under Contract F19628-00-C-0002. Opinions, interpretations, conclusions, and recommendations are those of the author and are not necessarily endorsed by the United States Government.

J.E. Piou is with Lincoln Laboratory, Massachusetts Institute of Technology (MIT), 244 Wood Street, Lexington, MA 02420-9185 USA; phone:781-981-1077; fax:781-981-0427;e-mail: jepiou@ll.mit.edu

carried on the rows and columns of the output data, respectively. The location of the *i*th scatterer in the 2-D space is given by $\left(angle(s_i), angle(p_i)\right)$.

This paper presents a technique that provides direct state pairing based on the coupling between s_i and p_i. Once the pole pairs $\left(s_i, p_i\right)$ are determined, the states can be paired. The complex amplitude may be extracted using a least-squares fit of a sum of poles, each weighted by a_i in the form of Eq. (1). Section III presents the two MIMO systems that give rise to the 2-D system realization algorithm.

III. MIMO SYSTEMS

Based on the 2-D data formulation defined by Eq. (1), the matrix notation of *M* measurements taken at *N* looks may be written

$$Y = \begin{bmatrix} y(1,1) & \cdots & y(1,N) \\ y(2,1) & \cdots & y(2,N) \\ \vdots & \cdots & \vdots \\ y(M-1,1) & \cdots & y(M-1,N) \\ y(M,1) & \cdots & y(M,N) \end{bmatrix}. \quad (3)$$

Thus one can form Hankel matrices with every row and column of the data matrix, which is defined by Eq. (3). For example, the Hankel matrices of the *m*th row and *n*th column are given by

$$H_m^{row} = \begin{bmatrix} y(m,1) & \cdots & y(m,L) \\ y(m,2) & \cdots & y(m,L+1) \\ \vdots & & \vdots \\ y(m,N-L+1) & \cdots & y(m,N) \end{bmatrix} \quad (4)$$

and

$$H_n^{col} = \begin{bmatrix} y(1,n) & \cdots & y(J,n) \\ y(2,n) & \cdots & y(J+1,n) \\ \vdots & & \vdots \\ y(M-J+1,n) & \cdots & y(M,n) \end{bmatrix}, \quad (5)$$

respectively. Parameters L and J that appear in Eqs. (4) and (5), respectively, denote the correlation windows in column and row directions. They are heuristically chosen to be $L = \lfloor N/2 \rfloor$ and $J = \lfloor M/2 \rfloor$, where the brackets denote the smallest integer less than or equal to the inserted quantity.

The primary interest in this section is modeling 2-D data by using two sets of complex matrices. The first set is derived from a MIMO system carried on a row-enhanced data matrix H^{row} with H_m^{row}; $m = 1, \cdots, M$ as entries. The second set of matrices is obtained from a MIMO system derived from a column-enhanced data matrix H^{col} with H_n^{col}; $n = 1, \cdots, N$ as matrix elements. Next, the two systems are coupled to obtain the 2-D system realization algorithm.

The row-enhanced data matrix can be obtained by stacking the *M* Hankel matrices described by Eq. (4) into a column vector such that

$$H^{\text{row}} = \begin{bmatrix} H_1^{\text{row}} \\ H_2^{\text{row}} \\ \vdots \\ H_M^{\text{row}} \end{bmatrix}. \quad (6)$$

Once an enhanced data matrix is defined, an autoregressive moving average (ARMA) model may be derived. The first MIMO system proposed may be seen as a relationship between an impulse matrix W_k^r and H_k^{row} and may be characterized by the ARMA recursive equation

$$H_k^{row} = \sum_{l=1}^{L_1} A_l H_{k-l}^{row} + \sum_{l=1}^{L_2} B_l W_{k-l}^r + B_0 W_k^r, \quad (7)$$

where A_l, B_l, and B_0 refer to the matrix coefficients of the ARMA model.

A single-input single-output (SISO) system of an ARMA characterizing Eq. (7) was developed in Reference [1], represented by a set of state variables [1,3]. Therefore, the ARMA model that is defined by Eq. (7) allows the following state-space representation:

$$X_{k+1}^r = A_r X_k^r + B_r W_k^r \quad (8)$$

and

$$H_k^{row} = C_r X_k^r + D_r W_k^r, \quad (9)$$

where $X_k^r \in \mathbf{C}^{P \times L}$ is the state, and $W_k^r \in \mathbf{C}^{L \times L}$ denotes the input with Dirac functions as entries on its main diagonal and zero elsewhere; $A_r \in \mathbf{C}^{P \times P}$, $B_r \in \mathbf{C}^{P \times L}$, $C_r \in \mathbf{C}^{(N-L+1) \times P}$ and $D_r \in \mathbf{C}^{(N-L+1) \times L}$ are constant matrices. Following the steps described in References [1,3], it is easy to see that

$$H_0^{\text{row}} \equiv D_r \quad (10)$$

and

$$H_k^{\text{row}} = C_r A_r^{k-1} B_r; \; k = 1, \cdots, M. \quad (11)$$

Eq. (11) indicates that an enhanced Hankel matrix H_e^{row} formed from a sequence of impulse matrix responses such that

$$H_e^{\text{row}} = \begin{bmatrix} H_1^{\text{row}} & H_2^{\text{row}} & \cdots & H_J^{\text{row}} \\ H_2^{\text{row}} & H_3^{\text{row}} & \cdots & H_{J+1}^{\text{row}} \\ \vdots & \vdots & \cdots & \vdots \\ H_{M-J+1}^{\text{row}} & H_{M-J+2}^{\text{row}} & \cdots & H_M^{\text{row}} \end{bmatrix} \quad (12)$$

can be factored. The decomposition of H_e^{row} into a product of two matrices is given by

$$H_e^{\text{row}} = \Omega\Gamma \quad (13)$$

where

$$\Omega = \begin{bmatrix} C_r \\ C_r A_r \\ \vdots \\ C_r A_r^{M-J} \end{bmatrix} \quad (14)$$

and

$$\Gamma = \begin{bmatrix} B_r & A_r B_r & \cdots & A_r^{J-1} B_r \end{bmatrix} \quad . \quad (15)$$

In linear system and control theory, Ω and Γ are known as the observability and controllability matrices, respectively. By computing the singular value decomposition of the enhanced Hankel matrix H_e^{row} and its low rank truncation [1,3] for a SISO system, the following P rank reduction of H_e^{row} is obtained:

$$\tilde{H}_e^{row} = U_{sn}\Sigma_{sn}V_{sn}^* . \quad (16)$$

In Eq. (16), U_{sn} denotes the signal components of the left-unitary matrix (U), and Σ_{sn} is a diagonal matrix with the signal singular values of H_e^{row} arranged in decreasing order as entries on its main diagonal. Furthermore, V_{sn} is the signal component of the right-unitary matrix (V) and $*$ denotes conjugate and transpose. Therefore, the observability and controllability matrices are given by

$$\Omega = U_{sn}\Sigma_{sn}^{1/2} \quad (17)$$

and

$$\Gamma = \Sigma_{sn}^{1/2}V_{sn}^* \quad . \quad (18)$$

respectively. Based on the results presented in Reference [4], the set of complex matrices (A_r, B_r, C_r) of the first MIMO system described by Eqs. (8) and (9) may be derived from Ω or Γ. First, the derivation of these matrices are based on Ω; they may be written

$$A_r = \left(\Omega_{-rl}^*\Omega_{-rl}\right)^{-1}\Omega_{-rl}^*\Omega_{-r1} \quad (19)$$

$$B_r = \left(\Omega_M^*\Omega_M\right)^{-1}\Omega_M^* H^{\text{row}} \quad (20)$$

$$C_r = \Omega(1\colon N-L+1,:) \quad , \quad (21)$$

where H^{row} is defined by Eq. (6) and

$$\Omega_{-r1} = \Omega(N-L+2\colon(M-J+1)(N-L+1),:) \quad (22)$$

$$\Omega_{-rl} = \Omega(1\colon(M-J)(N-L+1),:) \quad . \quad (23)$$

Ω_M is an extended observability matrix that is defined by

$$\Omega_M = \begin{bmatrix} C_r \\ C_r A_r \\ \vdots \\ C_r A_r^{M-1} \end{bmatrix} \quad . \quad (24)$$

In Eqs. (21) through (23), $\Omega(k\colon l,:)$ denotes the matrix obtained by keeping the rows k to l of Ω. The state-space matrices defined by Eqs. (19) through (21) may also be derived from the controllability matrix Γ. It is easy to see that

$$A_r = \Gamma_{-c1}\Gamma_{-cl}^*\left(\Gamma_{-c1}\Gamma_{-cl}^*\right)^{-1} \quad (25)$$

$$B_r = \Gamma(:,1\colon L) \quad (26)$$

$$C_r = H^{row}\Gamma_M^*(\Gamma_M\Gamma_M^*)^{-1} \quad , \quad (27)$$

where

$$\Gamma_{-c1} = \Gamma(:, L+1\colon LJ) \quad (28)$$

$$\Gamma_{-cl} = \Gamma(:,1\colon L(J-1)) \quad , \quad (29)$$

and where Γ_M is an extended controllability matrix that is defined by

$$\Gamma_M = \begin{bmatrix} B_r & A_r B_r & \cdots & A_r^{M-1} B_r \end{bmatrix} \quad . \quad (30)$$

In Eqs. (28) and (30), $\Gamma(:,k\colon l)$ refers to the matrix obtained by keeping the columns k to l of Γ. The column-enhanced data matrix H^{col} is formed by stacking the N Hankel matrices described by Eq. (5) into a row vector. Mathematically,

$$H^{col} = \begin{bmatrix} H_1^{col} & H_2^{col} & \cdots & H_N^{col} \end{bmatrix}. \quad (31)$$

The second MIMO system is derived from H^{col} by following steps similar to those described in Eqs. (7) through (18). The set of complex matrices (A_c, B_c, C_c) can be obtained from Ω by using Eqs. (19) through (21) or Γ by following Eqs. (25) through (27). The two MIMO systems are ready to be coupled. The coupled 1-D systems that give rise to the 2-D system realization algorithm are presented next.

IV. COUPLED 1-D SYSTEM REALIZATION

A technique to pair the eigenvalues s_i and p_i that are associated with the ith scatterer is presented here. This eigenvalue-pairing technique is based on the eigenvalue decomposition of the open-loop matrix A_r [which can be computed from Eq. (19) or (25)] of the first MIMO system.

The modal matrix of A_r will be used to reorder the eigenvalues of A_c.

The eigenvalue decomposition of A_r is written

$$\Lambda_r = M_r^{-1} A_r M_r \quad , \tag{32}$$

where Λ_r is a diagonal matrix with the eigenvalues of A_r defined by

$$\gamma\{A_r\} = \{s_1, s_2, \quad \cdots, s_P\} \tag{33}$$

as entries on its main diagonal. In Eq. (32) M_r denotes the modal matrix of A_r and is written

$$M_r = [v_1, v_2, \cdots, v_P] \quad , \tag{34}$$

where v_i represents the *i*th eigenvector associated with the eigenvalue s_i. Matrix A_{rc} is formed and defined by

$$A_{rc} = M_r^{-1} A_c M_r \quad . \tag{35}$$

The important elements of the preceding matrix are its diagonal entries, which are written

$$diag\{A_{rc}\} = \{A_{rc}(1,1), \cdots, A_{rc}(P,P)\} . \tag{36}$$

The eigenvalues of the second MIMO system are computed according to

$$\gamma\{A_c\} = \{\gamma_1, \gamma_2, \quad \cdots, \gamma_P\} \quad . \tag{37}$$

To associate the eigenvalues γ_i with their corresponding s_i, the reordering of the elements of $\gamma\{A_c\}$ are defined with respect to the position and strength of the entries of $angle(diag\{A_{rc}\})$ by $\{\gamma\{A_c\}\}^{angle(diag\{A_{rc}\})}$. For example, if $angle(diag\{A_{rc}(k,k)\})$ (i.e., $1 \le k \le P$) is the strongest element of $angle(diag\{A_{rc}\})$, the *k*th entry of $\gamma\{A_c\}$ must be the element that exhibits the highest angle strength. The poles associated with Eq. (33) are obtained from Eq. (37) according to

$$\{\gamma_1, \gamma_2, \cdots, \gamma_P\}^{angle(diag\{A_{rc}\})} = \{p_1, p_2, \cdots, p_P\} . \tag{38}$$

Note that Eqs. (33) and (38) provide the correct eigenvalue pair (s_i, p_i) associated with the *i*th scattering center. Therefore to obtain the proper state pairing between X^r and X^c one only needs to reorder the latter according to Eq. (38).

The complex amplitude a_i associated with *i*th eigenvalue pair (s_i, p_i) can be regarded as the *i*th element of an amplitude vector that can be extracted using a least-squares fit of a sum of eigenvalues to the data set; it is treated elsewhere (Reference [4]).

The 2-D system realization technique is summarized in the following algorithm:

1) Form the row- /column-enhanced data matrix H_e^{row} / H_e^{col} by using Eq. (12) and compute the state matrices $(A_r)/(A_c)$, $(B_r)/(B_c)$ and $(C_r)/(C_c)$ from Ω by using Eqs. (19) through (21) or Γ using Eqs. (25) through (27).

2) Compute the eigenvalue decomposition of A_r by using Eq. (32) to obtain the complex poles s_i and the entries of $\mathrm{diag}\{A_{rc}\}$ according to Eqs. (33) and (36), respectively.

3) Compute the complex poles p_i according to Eq. (38) and reorder the states X^c.

V. EXAMPLE FROM STATIC-RANGE RADAR OUTPUT MEASUREMENTS

Static-range output measurements taken on the 1.6 m long monoconic reentry vehicle described in Reference [5] and shown in Figure 1(a) is considered to confirm the effectiveness of the 2-D system realization algorithm. For this experiment, focus was on a segment of

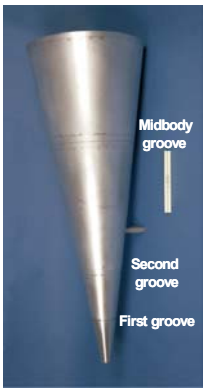

(a)

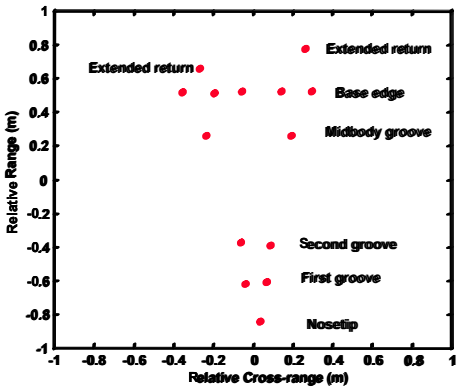

(b)

Figure 1. Canonical target (a) and phase plot of eigenvalues of 2-D system realization algorithm scaled to target relative physical dimensions; data used in (b) cover 1GHz bandwidth over 10 deg viewing angle.

1GHz data collected from 12–13 GHz in 40 MHz increments and a target viewing angle ranging from –5 to 5 deg in 0.25 deg step size. A model order of 14 (i.e., *P* = 14) is selected a priori to estimate the important features

(nosetip, grooves,and base edge) of the target. Figure 1(b) shows the 2-D phase plot of the pole pairs (s_i, p_i) scaled with respect to the relative target physical dimensions. The dots that describe the image of the target in the 2-D physical space are labeled to indicate the locations of the target features. Each groove in the image is defined by two scatterers (one at each edge), where the inner distance between them defines the relative diameter of the cone section wherein the groove is located. Furthermore, the algorithm represents the base edge by a set of four scatterers to indicate its strong contribution to the radar returns and the relative large diameter of the cone base. The two extended returns that appear in back of the base can be eliminated by choosing a smaller model order. However, the penalty for such a choice is a less accurate representation of the modeled data. As expected, in the image the nosetip is defined by only one scatterer.

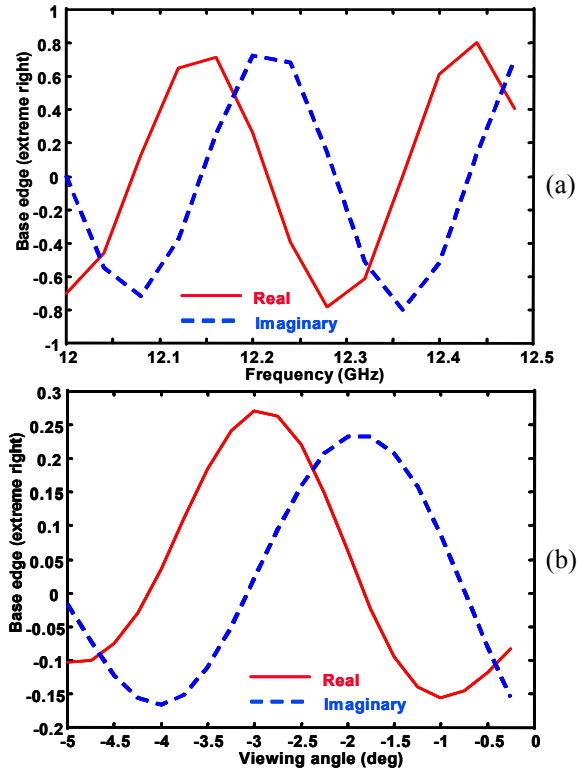

Figure 2. State response from base edge (extreme right scatterer) of canonical target for real (solid curve) and imaginary (dashed curve) components as a function of (a) Frequency and (b) viewing angle.

Figures 2(a) and (b) show the state associated to the base edge (extreme right scatterer) as a function of frequencies and viewing angles, respectively. The plots also show the real (solid curve) and imaginary (dashed curve) components of the state. The state associated with the nosetip is plotted in Figures (3). It is important to note that because of the heuristic choice of the correlation window length $L = \lfloor N/2 \rfloor$ and $J = \lfloor M/2 \rfloor$, the real and imaginary components for the states presented in Figures (2) and (3) are plotted only for half the frequency and angular extents. However, one can use the state matrices to cover the full bandwidth and viewing angle for the states related to the scattering centers.

The 17th column of the data matrix is chosen to compare the model obtained from the 2-D system realization algorithm and the measured data for a model order P = 14. Figures 4(a) and (b) illustrate the comparisons between the fit (dashed curve) and the data (solid curve) for the I and Q channels, respectively. In these figures the fitted model deviates from the measurements, primarily due to a low value of P. Next, the previous experiment is repeated using

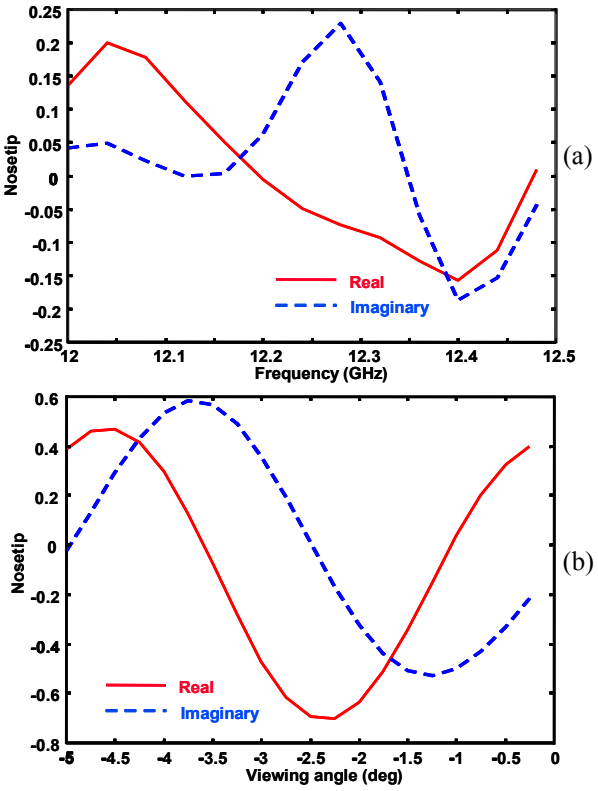

Figure 3. State response from nosetip of canonical target for real (solid curve) and imaginary (dashed curve) components as a function of (a) frequency and (b) viewing angle.

a model order P = 40. Figures 5(a) and (b) show excellent agreement between the model and the measured data. It is important to note that even though the high model order has the benefit of keeping the fitted data very close to the measurements, it is wise to have a trade-off between model order and the 2-D representation of the target in physical space.

VI. CONCLUSIONS

A two-dimensional system realization technique based on enhanced data matrices has been derived to extract state-space matrices in the row and column directions of a measurement matrix—states associated with the main scattering centers that form a target. The technique is computationally efficient because an algebraic method is used to couple the two sets of matrices. Static-range radar measurements taken on a canonical target have been used to judge the practicability of the algorithm. It has been demonstrated that when enhanced data matrices are used, the 2-D system realization technique provides accurate locations of the scattering centers and very good agreement between the fitted model and the matrix of measurements.

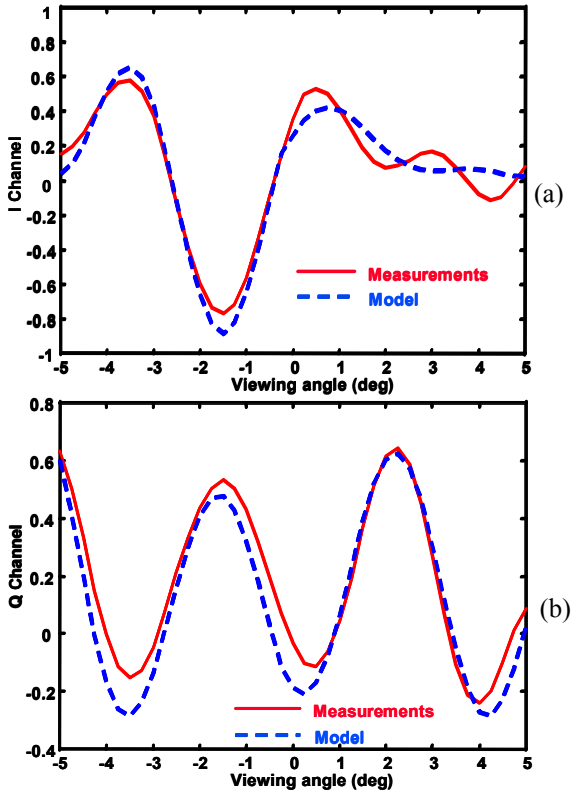

Figure 4. Comparison of fitted model (dashed curve), using an order P = 14, and measurements (solid curve) for 17th column of data matrix (a) real and (b) imaginary components .

REFERENCES

[1] S.Y. Kung, K.S. Arun, and D.V.B. Rao, "State-Space and Singular Value Decomposition-Based Approximation Methods for the Harmonic Retrieval Problem," *J. Opt. Soc. Am.*, 73, 1799–1811 (December 1983).

[2] Y. Hua, "Estimating Two-Dimensional Frequencies by Matrix Enhancement and Matrix Pencil," *IEEE Trans. Acoust., Speech, Signal Process.*, 40, 2267–ptember 1992).

[3] J.E. Piou, K.M. Cuomo, and J.T. Mayhan, "A State-Space Technique for Ultrawide-Bandwidth Coherent Processing," MIT Lincoln Laboratory, Lexington, Mass., Technical Rep. TR 1054 (20 July 1999), ESC-TR98-066.

[4] J.E. Piou, J.T. Mayhan, and K.M. Cuomo, "Algorithm Development and Performance Bounds for Sparse-Band, Sparse-Angle Processing," MIT Lincoln Laboratory, Lexington, Mass., Project Rep. NTP-4 (14 June 2001).

[5] K.M. Cuomo,J.E. Piou, and J.T. Mayhan, "Ultrawide-Band Coherent Processing," *IEEE Trans. Antennas Propag.*, 47, 1094-1107 (June 1999).

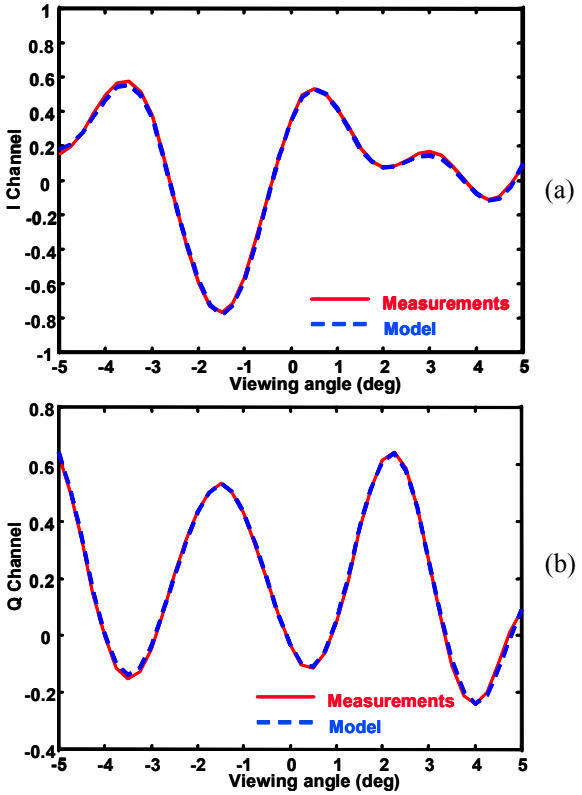

Figure 5. Comparison of fitted model (dashed curve), using an order P = 40, and measurements (solid curve) for 17th column of data matrix (a) real and (b) imaginary components.